



Cite this: *Chem. Commun.*, 2019, 55, 14665

Received 21st October 2019,
Accepted 14th November 2019

DOI: 10.1039/c9cc08261a

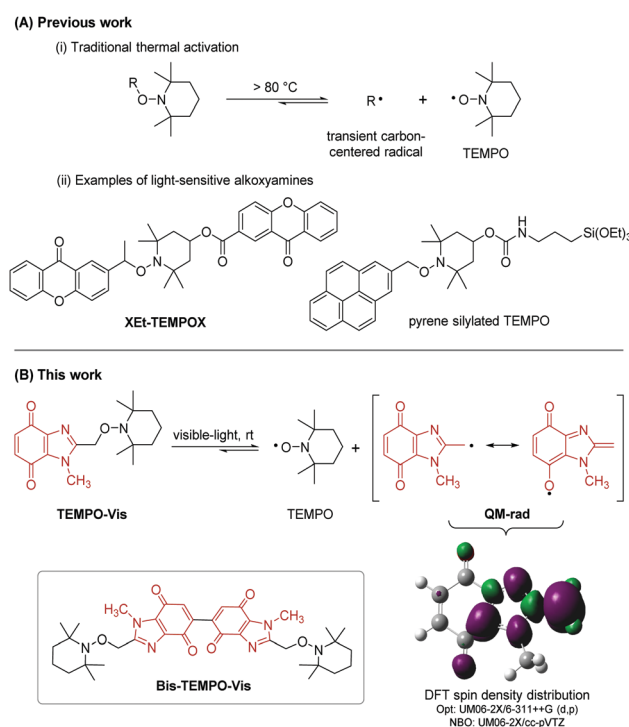
rsc.li/chemcomm

Visible-light unmasking of heterocyclic quinone methide radicals from alkoxyamines†

Patrick Kielty,^a Pau Farràs,^{ab} Patrick McArdle,^a Dennis A. Smith^a and Fawaz Aldabbagh^{id} *^{ac}

In nature, the unmasking of heterocyclic quinones to form stabilized quinone methide radicals is achieved using reductases (bioreduction). Herein, an alternative controllable room-temperature, visible-light activated protocol using alkoxyamines and bis-alkoxyamines is provided. Selective synthetic modification of the bis-alkoxyamine, allowed chromophore deactivation to give one labile alkoxyamine moiety.

Nitroxides are bench-stable free radicals and anti-oxidants with a broad range of applications. The most widely used is commercial (2,2,6,6-tetramethylpiperidin-1-yl)oxyl (TEMPO) with applications in synthesis and catalysis,^{1a} spin labelling,^{1b} magnetic resonance imaging (MRI),^{1c} fluorescence,^{1d} electrochemistry,^{1e} high-tech polymers,^{1f} and radical scavenging.^{1g} Nitroxides mask reactive carbon-centered radicals in the form of alkoxyamines. Homolysis of alkoxyamines is traditionally achieved *via* thermal activation, which for TEMPO usually requires temperatures above 80 °C (Scheme 1A).² The high temperature reversible trapping of initiator-derived alkyl and polymer radicals by nitroxide, is a process made popular by controlled/living nitroxide-mediated polymerization (NMP).³ There are examples of NMP using UV-light driven photodissociation of alkoxyamines.⁴ From a biomedical applications perspective, alkoxyamine activation at or near physiological temperature is essential. Low or ambient temperature activation using UV/visible-light has been reported using alkoxyamine derivatives of 4-hydroxy-TEMPO (4-OH-TEMPO),^{4c,5} including XET-TEMPO.^{5c} Guillauneuf and co-workers coupled benzylic derivatives of naphthalene, benzophenone, coumarin, anthraquinone and pyrene with 4-OH-TEMPO to give a series of UV/visible-light sensitive



Scheme 1 (A) Literature alkoxyamines (B) DFT-predicted controllable unmasking of heterocyclic quinone methide radicals using visible-light.

alkoxyamines (including the silylated TEMPO derivative).^{5b} For reported light-sensitive alkoxyamines,^{4c,5} the formation of thermodynamically stabilized benzylic radicals promotes the loss of TEMPO. Comparably, the generation of a quinone methide drives enzymatic bioreduction of mitomycin C (MMC) to allow aziridiny ring-opening and elimination of the carbamate functionality to give reactive sites for cross-linking with DNA.⁶ Benzimidazolequinone anti-tumor alternatives to MMC have been designed as prodrugs to form quinone methide upon bioreduction,⁷ or with adjustment of pH.⁸ Herein, we introduce heterocyclic benzimidazolequinone-based alkoxyamines; the simplest is **TEMPO-Vis**, where visible-light activated homolysis is

^a School of Chemistry, National University of Ireland Galway, University Road, Galway, H91 TK33, Ireland

^b Energy Research Centre, Ryan Institute, National University of Ireland Galway, University Road, Galway, H91 CF50, Ireland

^c Department of Pharmacy, School of Life Sciences, Pharmacy and Chemistry, Kingston University, Penrhyn Road, Kingston upon Thames, KT1 2EE, UK.
E-mail: f.alabbagh@kingston.ac.uk

† Electronic supplementary information (ESI) available: Supporting figures and tables, experimental procedures and NMR spectra. CCDC 1948448. For ESI and crystallographic data in CIF or other electronic format see DOI: 10.1039/c9cc08261a



driven by the formation of a quinone methide-type radical (**QM-rad**), stabilized by resonance delocalization (Scheme 1B). Bis-alkoxyamines are described, and visible-light is used for the first time to release up to two equivalents of TEMPO per molecule, using **Bis-TEMPO-Vis**. Bis- or bifunctional alkoxyamine activation has only been previously achieved by thermal means (at 70–140 °C),^{3,9} which for non-TEMPO bis-alkoxyamines leads to nitroxide decomposition.^{9c}

The premise for this room temperature homolysis was obtained through DFT investigation of the level of delocalization of the unpaired electron in **QM-rad** (Fig. S1, ESI†). DFT supported the traditional resonance structures with a shortening of the 2C–CH₂ bond relative to **TEMPO-Vis**, indicating partial double bond character (Table S1, ESI†), and significant distribution of spin density into the benzimidazolequinone ring system, including onto the quinone 7O-atom. The bond dissociation energy (BDE), and the lowest triplet energy level (E_T) of **TEMPO-Vis** were estimated using DFT. The model-alkoxyamine (**TEMPO-Vis**) was found to have a suitably low BDE (85.1 kJ mol^{−1}) compared to benzylic thermally labile (92.7–108.7 kJ mol^{−1}),¹⁰ and UV-light activated (80–122 kJ mol^{−1})^{4a} alkoxyamines, with enough driving force in the E_T to support the observed bond dissociation: $\Delta G_d = \text{BDE} - E_T = -122.3 \text{ kJ mol}^{-1}$ (see later discussion).

The preparation of **TEMPO-Vis** and **Bis-TEMPO-Vis** from 4,7-dimethoxybenzimidazole alkoxyamine precursor **1**, using one-step oxidation was investigated (Table 1). Previous work used NBS in combination with H₂SO₄ to convert 4,7-dimethoxybenzimidazole into benzimidazolequinone.¹¹ In the present work, **TEMPO-Vis** was isolated in 52% yield, with some undesirable bromination of **1** observed. PIFA [(CF₃CO₂)₂IPh] improved the yield of **TEMPO-Vis** to 78%. Oxidative dimerization of dimethoxybenzenes to dibenzoquinones is reported through the use of CAN [Ce(NH₄)₂(NO₃)₆],¹² and one report exists of a benzimidazolequinone dimer in low yield.¹³ Treatment of **1** with CAN (2 equiv.) afforded bis-alkoxyamine **2** in 86% yield, as the product of oxidative coupling of dimethoxybenzimidazole **TEMPO-Vis** with dimethoxybenzimidazole **1**. Increased amounts of CAN (3.2 equiv.) gave the fully oxidized **Bis-TEMPO-Vis** in 82% yield. The selective dimerization at C5–C5' was confirmed by X-ray crystallography of **Bis-TEMPO-Vis**, with alternative couplings at C6–C6', C5–C6' and C6–C5' not observed (Table 1).

To investigate the necessity in **Bis-TEMPO-Vis** of the benzimidazolequinone chromophore for the release of both attached TEMPO residues, a selective epoxidation strategy was devised for single chromophore deactivation (Scheme 2). Given its asymmetric aromatic/non-aromatic nature, **2** was deemed a good substrate for selective quinone functionalization. Subjecting **2** to the Langlois reaction (using NaSO₂CF₃),¹⁴ gave the electrophilic trifluoromethylated quinone bis-alkoxyamine **3** in 54% yield. The oxidative demethylation of **3** using NBS and H₂SO₄ (using Table 1 conditions), followed by mild epoxidation at the CF₃-containing quinone moiety, *via* air oxidation under basic conditions, furnished epoxide-quinone **4** in 78% yield.

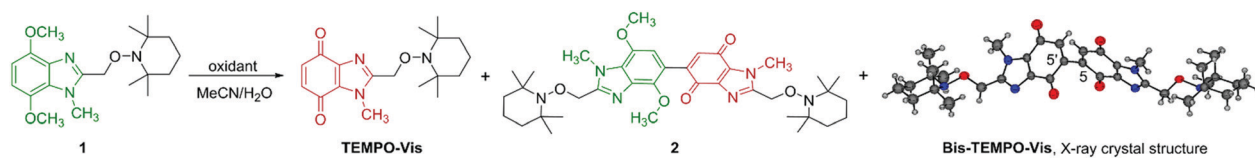
Visible-light activated alkoxyamine homolysis was carried out under an O₂ atmosphere to trap carbon-centered radicals,^{4a,5b,15} while monitoring alkoxyamine decay and TEMPO release by HPLC (Table 2).^{9b,16} Under blue LED (420–520 nm), 87% conversion of **TEMPO-Vis** to TEMPO was observed after 2.25 min. The decay of **TEMPO-Vis** alkoxyamine was first-order (Fig. 1A), from which the dissociation rate constant (k_d) was determined, and corresponded to a half-life ($t_{1/2}$) of 6 s. By monitoring [TEMPO] growth over time (Fig. 1B), eqn (1) may be fitted to the plot, to provide an alternative method to determine k_d , which also gave a $t_{1/2}$ of 6 s.

$$[\text{TEMPO}] = [\text{TEMPO}]_{\text{max}}(1 - e^{-k_d t}) \quad (1)$$

Alkoxyamines were indefinitely stable in the absence of light, and the on/off switchable nature of homolysis was demonstrated by alternating periods of light and dark for **TEMPO-Vis** using blue LED (Fig. S2, ESI†).

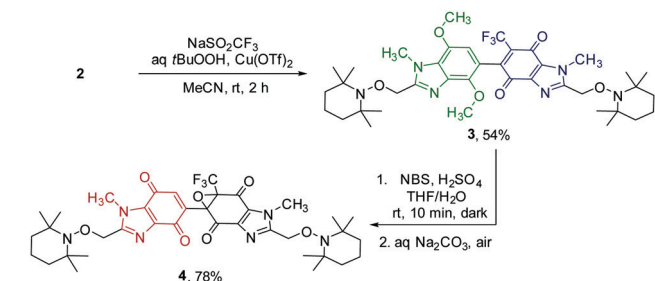
For the bis-alkoxyamine, **Bis-TEMPO-Vis**, there are two possible dissociation rate constants, k_{d1} and k_{d2} corresponding to TEMPO release from the starting compound, and from the monoalkoxyamine O₂-trapped intermediate(s), with hydroperoxide and aldehyde intermediates detected by HPLC-MS (Fig. S3, ESI†). Just over twice as much TEMPO was released from **Bis-TEMPO-Vis** compared to **TEMPO-Vis**, with 175% released after the same period of 2.25 min. The k_{d1} was directly measured from the first-order decay plot of **Bis-TEMPO-Vis**, and corresponded to a $t_{1/2}$ of 15 s in blue LED. The slower photolysis of **Bis-TEMPO-Vis** was supported by the DFT-derived ΔG_d being 11.7 kJ mol^{−1} less favorable compared to **TEMPO-Vis** (Table 2). The rate of overall TEMPO release attained by fitting eqn (1) to the [TEMPO] vs. time plot (Fig. 1B),

Table 1 Oxidation of dimethoxybenzimidazoles to visible-light sensitive benzimidazolequinone-alkoxyamines^{a,b}

				
Oxidant	Equiv.	TEMPO-Vis (%)	2 (%)	Bis-TEMPO-Vis (%)
NBS ^c	1.1	52 ^d	—	—
PIFA ^e	1.5	78	—	—
CAN ^f	2.0	—	86	—
CAN ^f	3.2	—	—	82

^a Isolated yields. ^b Performed in the absence of light. ^c H₂SO₄ (1.7 equiv.), THF/H₂O, rt, 10 min. ^d Brominated **1** and recovered **1** detected by HPLC-MS. ^e rt, 3 h. ^f 0 °C, 20 min.





Scheme 2 Chromophore deactivation.

combines release from the starting bis-alkoxyamine (k_{d1}), as well as from the O_2 -trapped intermediate alkoxyamine(s) (k_{d2}). The rate constant derived in this way was in good agreement with the rate of **Bis-TEMPO-Vis** decay (Fig. 1A and Table 2). This infers that for **Bis-TEMPO-Vis**, $k_{d1} \approx k_{d2}$, and the homolysis of the alkoxyamine in the O_2 -trapped intermediate(s) occurs at an almost identical rate to that of the starting bis-alkoxyamine.

By removing one of the chromophores of **Bis-TEMPO-Vis** in epoxide-quinone **4**, the release of <1 equiv. TEMPO occurred over the same time period (Table 2). The homolysis of one alkoxyamine of **4** was detected by HPLC-MS, with singly-homolyzed O_2 -trapped adducts observed (Fig. S3, ESI[†]), and no products of double alkoxyamine homolysis detected. Single bond homolysis occurred despite the BDE of the alkoxyamine of the epoxide part mirroring the BDE of **Bis-TEMPO-Vis**. TD-DFT calculations (see below) supported the localization of the frontier molecular orbitals on only the fully-conjugated quinone moiety of **4** (Fig. 2). The k_d of the labile alkoxyamine of **4** is less than half that of **Bis-TEMPO-Vis** in blue LED, and given that the ΔG_d values of the quinone-alkoxyamine in **4** and **Bis-TEMPO-Vis** are similar (at about -110 kJ mol⁻¹), the observed reduction in rate may be attributed to the lower absorption of the partially deactivated **4** in the visible region (Fig. S4, ESI[†]).

The rate of homolysis decreased using green (470–600 nm) compared to blue LED by 71-, 19- and 40-fold for **TEMPO-Vis**, **Bis-TEMPO-Vis**, and **4** respectively (Fig. S5, ESI[†]), due to less absorption. The decrease in absorbance is reflected in reduced quantum yields (Φ_h) with the greater intensity green LED used

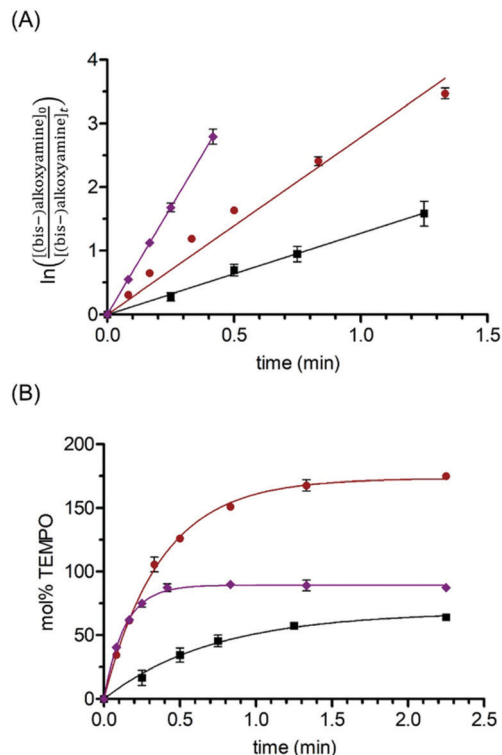


Fig. 1 Kinetics (at rt) of alkoxyamine and bis-alkoxyamine homolysis in blue LED according to (A) (bis-)alkoxyamine decay and (B) TEMPO release. Eqn (1) was fitted to the plots in (B) using GraphPad Prism software. Key: **TEMPO-Vis** (—●—), **Bis-TEMPO-Vis** (—●—) and **4** (—■—). Conditions according to Table 2.

(see Table S2, ESI[†]). Moreover, **Bis-TEMPO-Vis** underwent photolysis at a faster rate than **TEMPO-Vis** in green LED, in accordance with λ_{max} of the former being red-shifted by 12 nm (Fig. S4, ESI[†]). The result in green LED, is a reversal in the magnitude of k_d that was observed for blue LED for the two compounds. The same conclusion of $k_{d1} \approx k_{d2}$ for **Bis-TEMPO-Vis** was reached for green LED activation.

Bis-alkoxyamine **2** was found to be largely stable under visible-light, having a k_d three orders of magnitude smaller than its fully-oxidized derivative, **Bis-TEMPO-Vis**, in blue and green LED (Table 2). Although **2** possesses a similar first BDE to

Table 2 Kinetics for room-temperature alkoxyamine homolysis under visible-light,^a and DFT-calculated homolysis parameters

Alkoxyamine	LED color	k_d^b via alkoxyamine decay (min ⁻¹)	k_d^c via TEMPO release (min ⁻¹)	mol% ^d TEMPO released (time, min)	BDE ^e (kJ mol ⁻¹)	E_T^e (kJ mol ⁻¹)
TEMPO-Vis	Blue	6.71 ± 0.21	7.29 ± 0.26	87 (2.25)	85.1	207.4
Bis-TEMPO-Vis	Blue	2.78 ± 0.07	2.66 ± 0.09	175 (2.25)	104.9	215.5
4	Blue	1.27 ± 0.16	1.41 ± 0.24	64 (2.25)	99.7, ^f 104.6 ^g	209.7
2	Blue	0.00313 ± 0.00055	0.00417 ± 0.00024	78 (480)	104.1, ^f 111.9 ^g	176.8
TEMPO-Vis	Green	0.0948 ± 0.0032	0.0993 ± 0.0063	80 (25)	—	—
Bis-TEMPO-Vis	Green	0.148 ± 0.002	0.146 ± 0.004	162 (15)	—	—
4	Green	0.0321 ± 0.0007	0.0346 ± 0.0061	43 (65)	—	—
2	Green	$<2 \times 10^{-4}$	—	<5 (480)	—	—

^a Conditions: alkoxyamine (0.25 mM, DCE) illuminated at rt using blue (1 × 9 W) or green (2 × 9 W) LED bulbs under O_2 balloon with HPLC analysis. Experiments performed in triplicate. ^b Dissociation rate (k_d) derived from slope of Fig. 1A and Fig. S5A (ESI). ^c Derived from fit of eqn (1) to Fig. 1B and Fig. S5B (ESI). ^d HPLC yield based on starting alkoxyamine. ^e M06-2X, or UM06-2X for radicals, 6-311++G (d,p) in the gas phase. ^f BDE at benzimidazolequinone part. ^g BDE at epoxide/dimethoxybenzimidazole part.



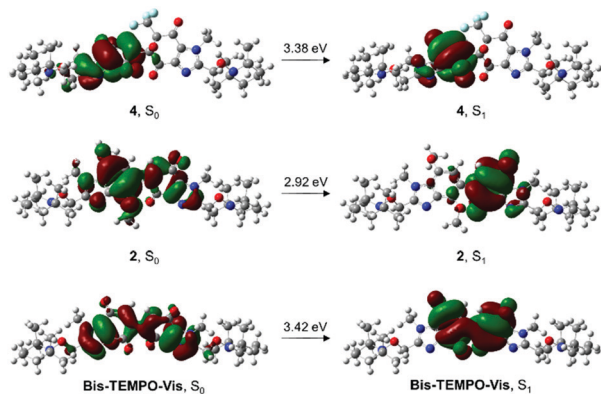


Fig. 2 TD-DFT analysis of ground and excited state orbital delocalization in epoxide-quinone **4**, *p*-dimethoxybenzene-coupled quinone **2**, and **Bis-TEMPO-Vis**. Conditions: PCM/M06-2X/6-311++G (d,p), using DCE as solvent and the natural transition orbital (NTO)¹⁷ method for visualization.

Bis-TEMPO-Vis, its E_T was more than 30 kJ mol⁻¹ lower than the other alkoxyamines. The λ_{max} of **2** was red-shifted by 96 nm compared to **Bis-TEMPO-Vis**, suggesting the presence of a low-lying charge-transfer (CT) state (Fig. S4, ESI[†]). Cyclic voltammetry on **2** and its constituent alkoxyamines **1** and **TEMPO-Vis**, supported the localization of the HOMO and LUMO to the dimethoxybenzimidazole and the benzimidazolequinone motifs respectively (Fig. S6, ESI[†]). Time-dependent density functional theory (TD-DFT)¹⁸ provided graphical representation of spatially-separated ground and excited state orbitals (Fig. 2). The ground state (S_0) of **2** is primarily localized on the dimethoxybenzimidazole, while the density of the first excited state (S_1) is entirely localized on the quinone, with limited overlap between the two states. In comparison, the CT effect is not observed in the analogous TD-DFT of **Bis-TEMPO-Vis**.

In conclusion, alkoxyamines of heterocyclic quinones are introduced with room temperature visible-light homolysis providing an alternative to nature's bioreductive activation of prodrugs, as a means of unmasking the transient quinone methide. This includes an alkoxyamine that can release up to two equivalents of nitroxide per molecule using visible-light activation, and that does so sequentially with $k_{d1} \approx k_{d2}$. Facile synthetic deactivation of one chromophore limited TEMPO release to <1 equiv. For blue LED, the rates of bond homolysis can largely be rationalized by thermodynamics, while for green LED variations in absorbance become more important. The placement of an electron-rich substituent on the electron-deficient quinone gives a charge-transfer state that stabilizes the quinone under visible-light. The benzimidazole-quinone alkoxyamines offer the possibility of wide-ranging applications from visible-light activated anti-tumour cytotoxins to radical initiators for vinyl monomer photopolymerizations giving polymers end-functionalized with antibiotics.

We thank the Irish Research Council for awarding PK an Enterprise Partnership Postgraduate Scholarship. We are grateful

to Peter Cannon (Avara Pharmaceutical Services Ltd., Shannon, Ireland) for acting as the Enterprise Mentor. PF acknowledges support from Royal Society Newton Alumni programme. We thank Sylvester Byrne and Benjamin A. Chalmers for laboratory assistance, and John O'Reilly for consultation on HPLC (all National University of Ireland Galway). Andrew Benniston (Newcastle University, UK) is gratefully acknowledged for discussions around the photophysical and computational studies.

Conflicts of interest

There are no conflicts to declare.

Notes and references

- (a) H. A. Beejapur, Q. Zhang, K. Hu, L. Zhu, J. Wang and Z. Ye, *ACS Catal.*, 2019, **9**, 2777; (b) M. M. Haugland, J. E. Lovett and E. A. Anderson, *Chem. Soc. Rev.*, 2018, **47**, 668; (c) J. Wahsner, E. M. Gale, A. Rodríguez-Rodríguez and P. Caravan, *Chem. Rev.*, 2019, **119**, 957; (d) A. Kaur, J. L. Kolanowski and E. J. New, *Angew. Chem., Int. Ed.*, 2016, **55**, 1602; (e) J. E. Nutting, M. Rafiee and S. S. Stahl, *Chem. Rev.*, 2018, **118**, 4834; (f) K.-A. Hansen and J. P. Blinco, *Polym. Chem.*, 2018, **9**, 1479; (g) E. G. Bagryanskaya and S. R. A. Marque, *Chem. Rev.*, 2014, **114**, 5011.
- T. Fukuda, T. Terauchi, A. Goto, K. Ohno, Y. Tsujii, T. Miyamoto, S. Kobatake and B. Yamada, *Macromolecules*, 1996, **29**, 6393.
- J. Nicolas, Y. Guillauneuf, C. Lefay, D. Bertin, D. Gigmes and B. Charleux, *Prog. Polym. Sci.*, 2013, **38**, 63.
- (a) D.-L. Versace, Y. Guillauneuf, D. Bertin, J. P. Fouassier, J. Lalevée and D. Gigmes, *Org. Biomol. Chem.*, 2011, **9**, 2892; (b) Y. Guillauneuf, D. Bertin, D. Gigmes, D.-L. Versace, J. Lalevée and J.-P. Fouassier, *Macromolecules*, 2010, **43**, 2204; (c) S. Hu, J. H. Malpert, X. Yang and D. C. Neckers, *Polymer*, 2000, **41**, 445.
- (a) A. Goto, J. C. Scaiano and L. Maretti, *Photochem. Photobiol. Sci.*, 2007, **6**, 833; (b) M. Baron, J. C. Morris, S. Telitel, J.-L. Clément, J. Lalevée, F. Morlet-Savary, A. Spangenberg, J.-P. Malval, O. Soppera, D. Gigmes and Y. Guillauneuf, *J. Am. Chem. Soc.*, 2018, **140**, 3339; (c) M. Herder and J.-M. Lehn, *J. Am. Chem. Soc.*, 2018, **140**, 7647.
- P. D. Bass, D. A. Gubler, T. C. Judd and R. M. Williams, *Chem. Rev.*, 2013, **113**, 6816.
- (a) W. G. Schulz, R. A. Nieman and E. B. Skibo, *Proc. Natl. Acad. Sci. U. S. A.*, 1995, **92**, 11854; (b) C. Flader, J. Liu and R. F. Borch, *J. Med. Chem.*, 2000, **43**, 3157.
- E. B. Skibo, *J. Org. Chem.*, 1992, **57**, 5874.
- (a) I. Q. Li, B. A. Howell, R. A. Koster and D. B. Priddy, *Macromolecules*, 1996, **29**, 8554; (b) G. Ananchenko and K. Matyjaszewski, *Macromolecules*, 2002, **35**, 8323; (c) J. Ruehl, N. L. Hill, E. D. Walter, G. Millhauser and R. Braslau, *Macromolecules*, 2008, **41**, 1972.
- J. L. Hodgson, L. B. Roskop, M. S. Gordon, C. Y. Lin and M. L. Coote, *J. Phys. Chem. A*, 2010, **114**, 10458.
- L. O'Donovan, M. P. Carty and F. Aldabbagh, *Chem. Commun.*, 2008, 5592.
- B. E. Love, J. Bonner-Stewart and L. A. Forrest, *Synlett*, 2009, 813.
- A. Gellis, H. Kovacic, N. Boufatah and P. Vanelle, *Eur. J. Med. Chem.*, 2008, **43**, 1858.
- B. R. Langlois, in *Modern Synthesis Processes and Reactivity of Fluorinated Compounds*, ed. H. Groult, F. R. Leroux and A. Tressaud, Elsevier, 2017, ch. 5, pp. 125.
- D. W. Grattan, D. J. Carlsson, J. A. Howard and D. M. Wiles, *Can. J. Chem.*, 1979, **57**, 2834.
- G. Moad and E. Rizzardo, *Macromolecules*, 1995, **28**, 8722.
- R. L. Martin, *J. Chem. Phys.*, 2003, **118**, 4775.
- A. D. Laurent and D. Jacquemin, *Int. J. Quantum Chem.*, 2013, **113**, 2019.

